Biophysical Journal, Volume *121*

Supplemental information

Competition for shared downstream signaling molecules establishes indirect negative feedback between EGFR and EphA2

Dongmyung Oh, Zhongwen Chen, Kabir H. Biswas, Funing Bai, Hui Ting Ong, Michael P. Sheetz, and Jay T. Groves

Single molecule kinetics equation

In ensemble population, the rate equation for protein A and B interaction is

$$\frac{d[A:B]}{dt} = k_{on}[A][B](t) - k_{off} \cdot [A:B](t) \ \ (Eq\ 1)$$

, where k_{on} and k_{off} are association and dissociation constant. Here, the concentration change can be measured directly *in vitro* system. However, in living cells, certain proteins interact simultaneously with many different species at different cellular locations, resulting in a big challenge in *in vivo* protein-protein reaction. However, using single molecule based counting data, this problem can be solved by replacing k_{on}[A][B](t) and k_{off} with the geometric rate function, $\gamma_{on}(t)$ and $\lambda_{off}(t)$, respectively (*1, 2*). In our system, the rate equation of Grb2 binding in the activated RTKs is

$$\frac{d[pYRTK_{complex}:Grb2]}{dt} = \gamma_{on}(t) - \lambda_{off}(t) \cdot [pYRTK_{complex}:Grb2](t) \ \ (Eq\ 2)$$

, where $pYRTK_{complex}$ represents ligand:RTK complex, and thus, ligand-induced phosphorylation of RTK in the cell membrane. Instead of k_{on}, $\gamma_{on}(t)$ carries information about the time-varying local concentration of reactants and is determined experimentally by molecule counting. We started a single molecule kinetics experiment at saturation of phosphorylated-EphA2 in ephrin-A1 coated-SLB. Therefore, finally, the time was set as the moment of the addition of EGF. In cell membrane, the dissociation rate function $\lambda_{off}(t)$ of Grb2 in pY-EGFR is related to the k_{on}, k_{off} and diffusion rate D, where D depends on clustering of phosphorylated-EGFR (*3*).

The complex [pYRTK$_{complex}$:Grb2](t) can be derived by solving the above nonlinear first-order differential equation (Eq2);

$$[pYRTK_{complex}:SH2](t) = ce^{-\int_{t=0}^{t}\lambda_{off}(t')\,dt'} + e^{-\int_{t=0}^{t}\lambda_{off}(t')dt'}\int_{t=0}^{t}\gamma_{on}(t') \cdot e^{\int_{t=0}^{t}\lambda_{off}(t')dt'}dt' (Eq3).$$

Finally, $\gamma_{on}(t)$ and $\lambda_{off}(t)$ rate functions can be determined using single molecule data and numerically plugged into Eq3 to obtain a time-dependent ligand:RTK:Grb2 complex. As described above, we determined $\gamma_{on}(t)$ as the number of new membrane binding event per time, and $\lambda_{off}(t)$ was determined by the reciprocal of the dwell time of molecules.

Remove free ephrin-A1 ligands in ephrin-A1:EphA2 clusters in SLB

Assuming there are still free ephrin-A1-Alexa 680 ligands in the ephrin-A1-Alexa 680 clusters regions in SLB, this unbounded ligand signal can be subtracted from the measured clusters fluorescence signal. The concept of uniformity of ephrin-A1-Alexa 680 distribution on the SLB and fluorescence signal density are used. For the entire SLB surface area, the total density of ephrin-A1-Alexa 680 fluorescence signal (I_{total}) was defined as the total fluorescence signal divided by the total SLB area (S_{total});

$$I_{total} = \frac{\sum_i^n k_i}{S_{total}}$$

The I_{total} was composed of clustered ($I_{cluster}$) and non-clustered ($I_{non\text{-}cluster}$) regions and which were directly measured with fluorescence image (Figure S3, ROI 1 and ROI 2);

$$I_{total} = I_{cluster} + I_{non-cluster}$$

$I_{cluster}$ was composed of EphA2-bound ligands ($I_{EphA2\text{-}bound}$) and free ligands (I_{free}), respectively;

$$I_{cluster} = \frac{\sum_i^n k_i}{S_{cluster}} = \frac{\sum_i^n \left(k_i^{EphA2-bound} + k_i^{free}\right)}{S_{cluster}} = I_{cluster}^{EphA2-bound} + I_{cluster}^{free}$$

,where $S_{cluster}$ represents the clustered area and k_i represents the pixel intensity of the clustered area. The k_i consists of k_i $^{\text{EphA2-bound}}$ and k_i $^{\text{free}}$ representing the pixel intensity of the EphA2-bound and free ephrin-A1-Alexa 680 signal, respectively. The density of the free ligands in the non-clustered region ($I_{non\text{-}cluster}$) (Figure S3 D, black) should be equal to the density of free ligands in clusters regions ($I_{cluster}^{free}$) due to the uniform distribution in SLB surface;

$$I_{non-cluster} = \frac{\sum_i^n k_i}{S_{non-cluster}} = \frac{\sum_i^n k_i^{free}}{S_{cluster}} = I_{cluster}^{free}$$

Thus, the relative amount of EphA2-bound ephA1-Alexa 680 become

$$\frac{I_{cluster}^{EphA2-bound}}{I_{total}} = 1 - 2 \cdot \left(\frac{I_{non-cluster}}{I_{total}}\right)$$

. The clustering ephA1-Alexa 680 signals calculated above in SLB (Figure S3 D, red) showed slightly faster dynamics than that before subtracting the free ligands signal (Figure S3 D, gray). However, the calculated ligand clustering dynamics showed more anti-symmetric behavior with the ephrin-A1 diffusing dynamics in non-clustered regions (Figure S3 D, black). Therefore, this analysis demonstrates the fluidity of SLB and free diffusion of ligand on the SLB surface.

Supporting Data

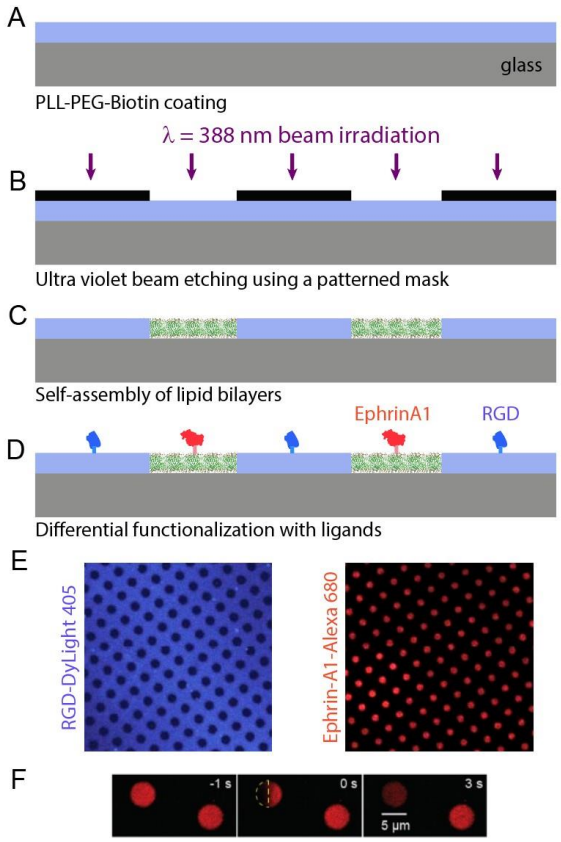

Figure S1. Protocol for micropatterned SLB hybrid substrates. (A) A cleaned coverslip is coated with PLL-(*g*)-PEG-biotin (50 %, Susos) for 2 hours. (B) UV (λ = 388 nm) etching of the PLL-(*g*)-PEG-biotin polymer coat with a micro-patterned photomask for 9 minutes following which, etched polymer was washed out using deionized water. (C) Incubation of the polymer-patterned substrate with lipid vesicles containing 4 % Ni-NTA-DOGS for 5 minutes for self-assembly of SLB corrals in the UV-etched regions of the substrate. (D) Micropatterned hybrid substrates were then functionalized with 1 µg/ml of either DyLight 405-NeutrAvidin or NeutrAvidin (Thermo-Fisher) through NeutrAvidin-biotin interaction with PLL-(*g*)-PEG-biotin, and with 5 nM of His-tagged ephrin-A1-Alexa 680 through His-tag-NiNTA interaction with Ni-NTA-DOGS lipid for 1 hour at room temperature. Substrates were further incubated with biotinylated cyclic RGD peptides to generate cyclic RGD-functionalized polymer surfaces. (E) Fluorescence images of a hybrid substrate with RGD (blue) and ephrin-A1 ligands (red). (F) Point-source fluorescence recovery after photobleaching (FRAP) of ephrin-A1-Alexa 680 in SLB. Recovery of ephrin-A1-Alexa 680 fluorescence within 3 s indicates that the protein was freely diffusing on the SLB surface.

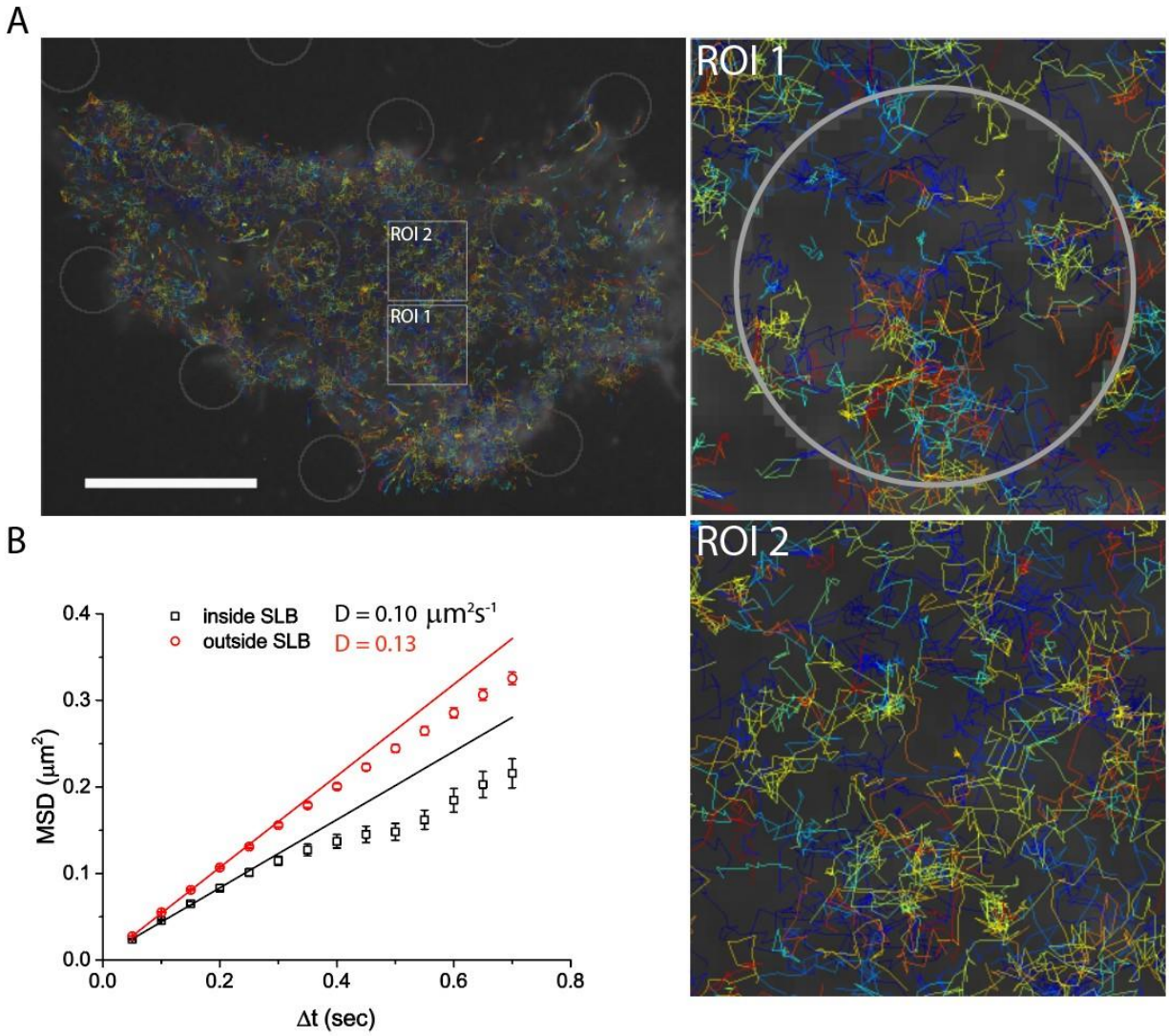

Figure S2. Ephrin-A1:EphA2 clusters in SLB do not interfere with EGFR motility. (A) Trajectories of individual EGFR-mEos3.2 in the bottom membrane of MDA-MB-231 cells. EGFR-mEos3.2 diffuses freely throughout the cell membrane, including SLBs regions (gray circles) where ephrin-A1 is present. Zoom images of ROI 1 and ROI 2, representing the SLB and the background region respectively, are shown next. (B) Mean squared displacement (MSD) versus time-lag (Δt) curves of EGFR-mEos3.2 trajectories found in the inner (black) and outer (red) SLBs. The first five data points fit with normal diffusion equation MSD = 4Dt, where D is the diffusion coefficient. Bar is 10 μm.

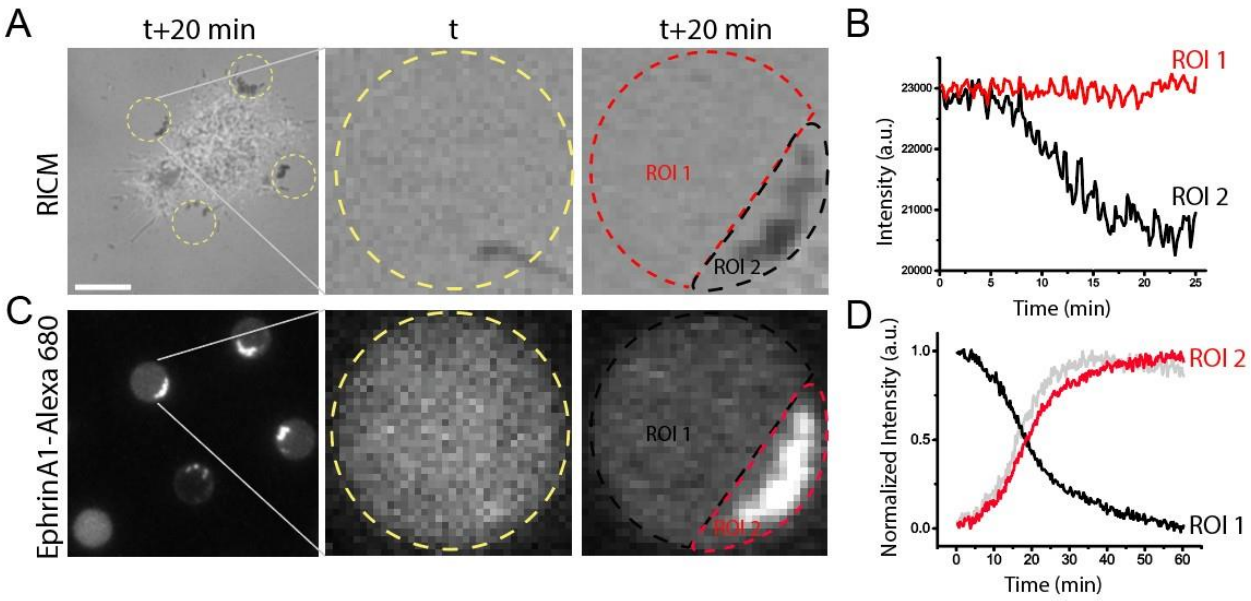

Figure S3. Ephrin-A1 clustering in cell-SLB contact. (A) RICM image of MDA-MB-231 cells spreading on the ephrin-A1-SLB patterned (yellow circles) substrate shows initial cell-SLB contact (middle) and strong adhesion for 20 min (third panel). (B) Time-lapse intensity profile of cell adhesion signal in SLB, partitioned with cell-contact (ROI 2) and non-contact regions (ROI 1). (C) Epifluorescence image of ephrin-A1-Alexa 680 shows ligand clustering at cell-SLB contact regions (ROI 2). (D) Normalized time-lapse intensity profiles of free ephrin-A1-Alxex 680 (ROI 1) and cell-contact region (ROI 2). The gray and red curves show the intensity profiles before (gray) and after (red) subtraction of the free ephrin-A1 intensity from clustered regions, respectively (see above supporting material), Scale bar, 5 µm.

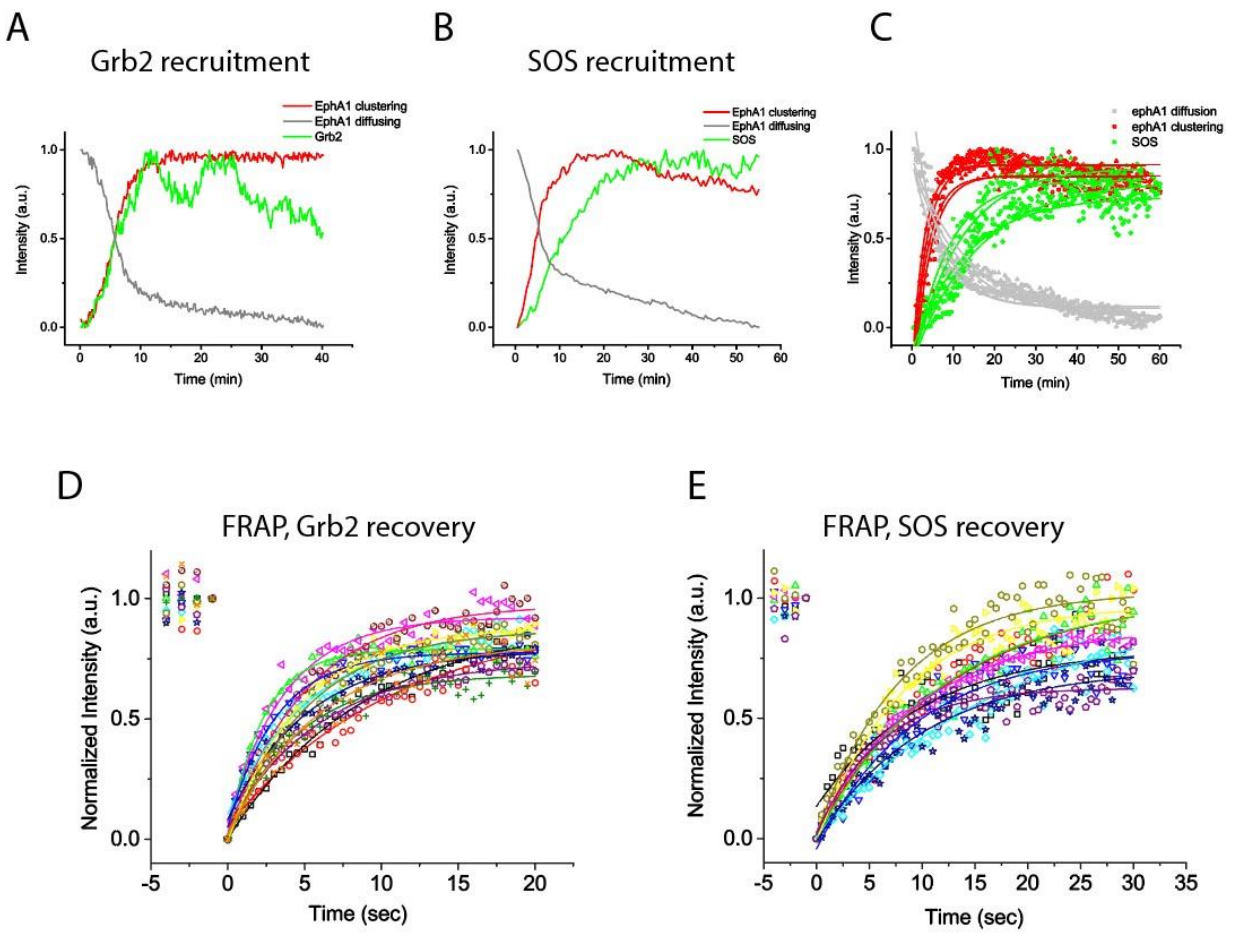

Figure S4. Immediate ephrin-A1:EphA2 recruitment of Grb2 but delayed recruitment of SOS. (A - C) Representative intensity profiles of ephrin-A1-Alexa 680 signal clustering in cell-SLB contact regions (red) and simultaneous ephrin-A1-Alexa 680 dissipation from outside clusters regions (gray) in SLB. Typical intensity profiles of Grb2-tdEos recruitment signal (green, in A) and SOS-mEos3.2 (green, in B - C) in ephrin-A1 clusters. (D - E) FRAP curves of Grb2-tdEos (D) (n = 16 cells) and SOS-mEos3.2 (E) (n = 14 cells) performed with a point-source laser beam that illuminates a partial region in the SLB (see Figure 2 C). Statistics were shown in Figure 2E. These data indicate that SOS recruitment and replacement for the ephrin-A1:EphA2 clusters occurs after Grb2 interaction.

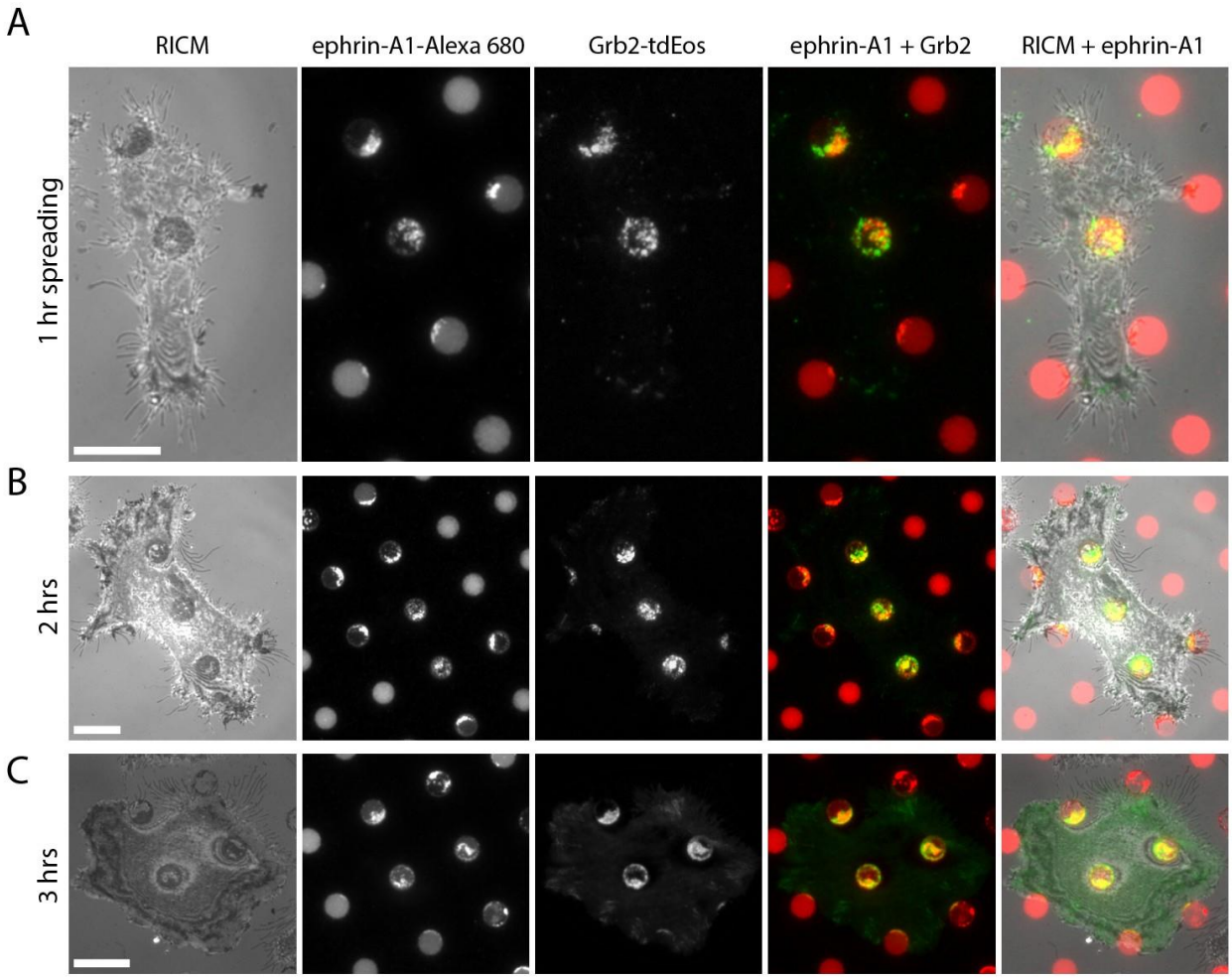

Figure S5. Sustained ephrin-A1:EphA2:Grb2 signaling in SLB. (A - C) MDA-MB-231 cells (first column) expressing Grb2-tdEos (third column) spread on the ephrin-A1-Alexa 680 coated SLB arrays (second column) for 1 hour (A), 2 hours (B), and 3 hours (C). Merged image of ephrin-A1-Alexa 680 and Grb2-tdEos (forth) and merged image of all channels (last) show persistent Grb2 localization with ephrin-A1 clusters formed on SLBs. Scale bars, 10 μm.

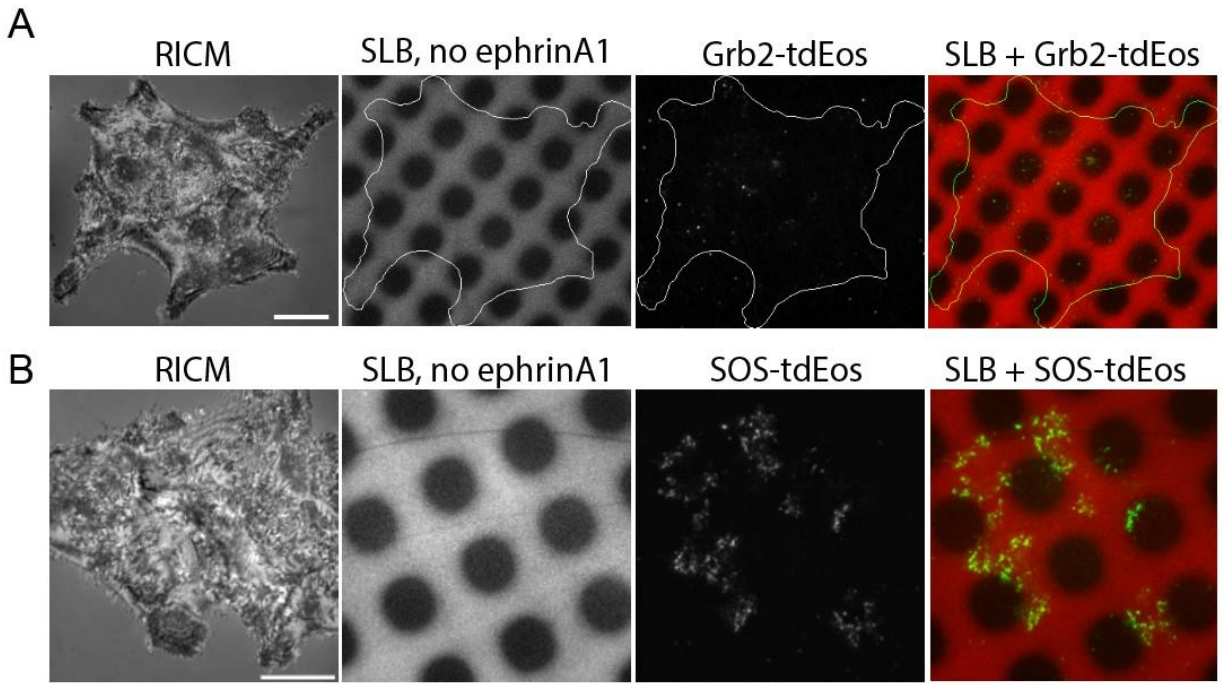

Figure S6. Ephrin-A1-dependent Grb2 and SOS recruitment in SLB. (A - B) RICM, epifluorescence, and TIRF images of MDA-MB-231 cells expressing either Grb2-tdEos (A, 3rd panel) and SOS-mEos3.2 (B, 3rd panel) and interacting with micropatterned substrates without ephrin-A1 ligands. SLB recruitment of Grb2-tdEos or SOS-mEos3.2 is limited, indicating restricted EphA2 activation in SLB regions. Scale bars, 10 µm.

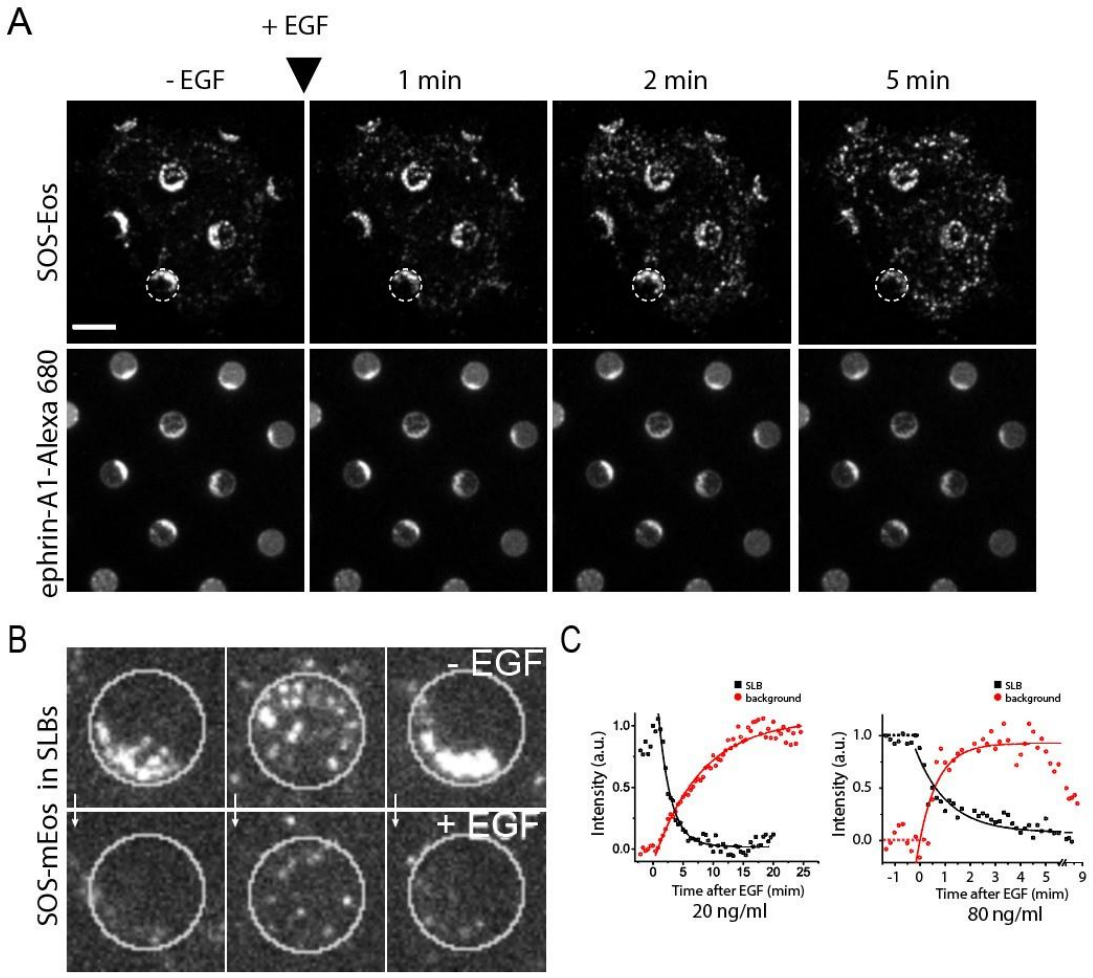

Figure S7. Competition between ligand activated EphA2 and EGFR receptors for SOS recruitment. (A) The time-lapse SOS-mEos3.2 images (in the green channel) before and after EGF (80 ng/ml) (full version, Movie 6) show a signal decrease in ephrin-A1 SLB regions but simultaneous increase in regions outside of SLBs (top row). Time-lapse ephrin-A1-Alexa 680 images shows similar intensity and cluster shape before and after EGF (bottom). Scale bar, 5 µm. (B) SLB collection from a cell highlighted SOS-mEos3.2 signal depletion from ephrin-A1:EphA2 after EGF stimulation (see Movie 7). (C) Corresponding normalized intensity profiles of SOS-mEos3.2 signals inside (black, ephrin-A1:EphA2 complex) and outside (red, equivalent to EGF:EGFR complex) of SLB corrals before ($t < 0$) and after EGF ($t > 0$) with 20 ng/ml (left) and 80 ng/ml of EGF (right). Exponential decay function fitting to the curves provides characteristic time constants of τ_{EphA2} = - 1.3 min (80 ng/ml EGF) and τ_{EphA2} = - 2.5 min (20 ng/ml EGF) inside SLBs and τ_{EGFR} = + 0.7 min (80 ng/ml EGF) and + 7.9 min (20 ng/ml EGF) outside SLBs respectively. A negative sign means a decrease in intensity. Scale bar, 5 µm.

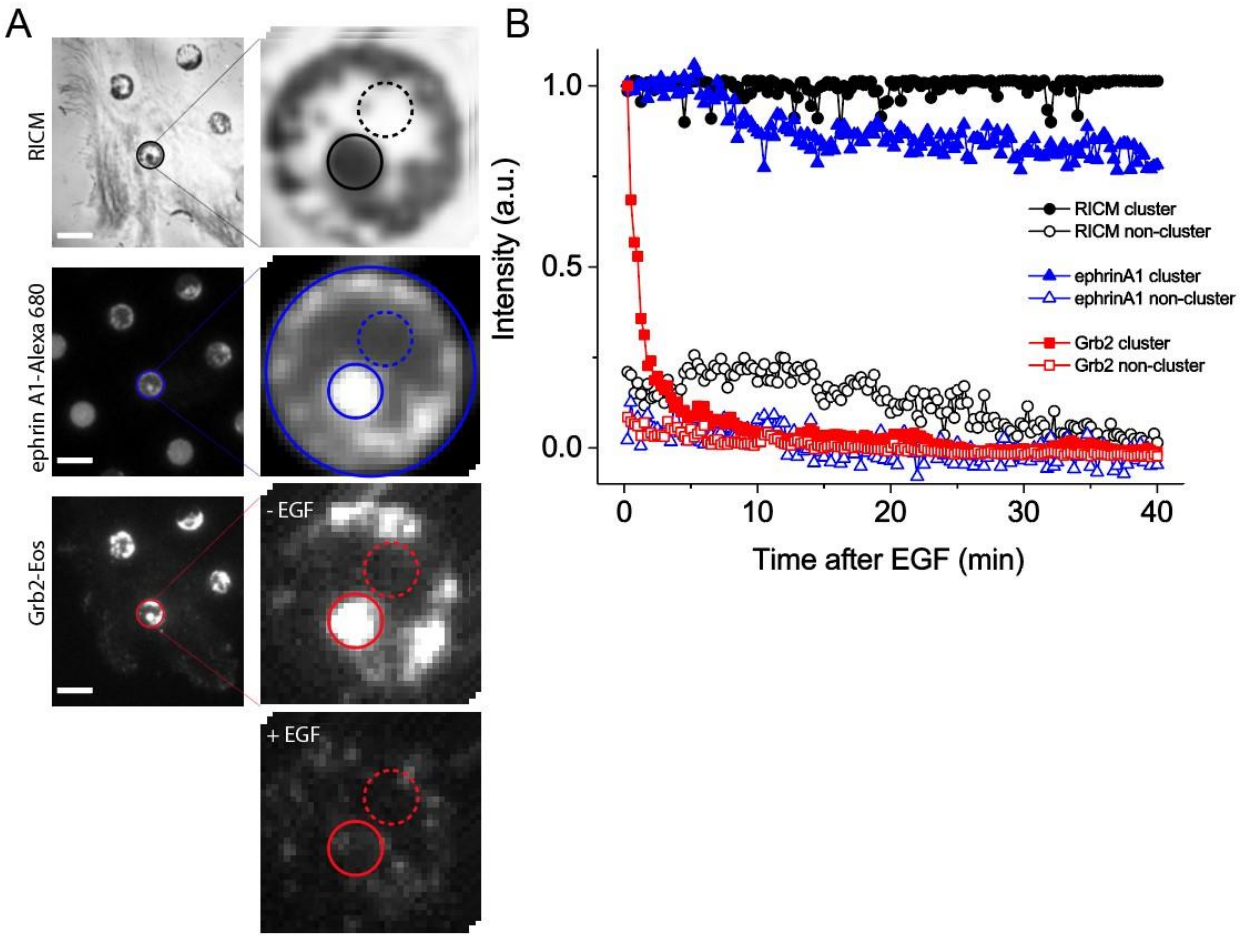

Figure S8. Depletion of the newly formed EGF:EGFR:Grb2 complexes in the ephrin-A1 SLBs. (A) RICM (first row) of MDA-MB-231 cell, epifluorescence image of ephrin-A1-Alexa 680 (second), and TIRF image of Grb2-tdEos before (third) and after EGF (forth). Corresponding zoom images of the SLB (left column) marked in A. (B) Intensity profiles of RICM (black), ephrin-A1-Alexa 689 (blue), and Grb2-tdEos (red) in ephrin-A1 clusters (closed symbols) and non-ephrin-A1 clusters (opened symbols) marked in the zoom images in A with solid and dotted circles respectively. Grb2-tdEos signal at the ephrin-A1 clusters was significantly reduced as expected, but no detectable signal changes in non-ephrin-A1 clusters was found, indicating the limited formation of EGF:EGFR:Grb2 complex in SLB corrals.

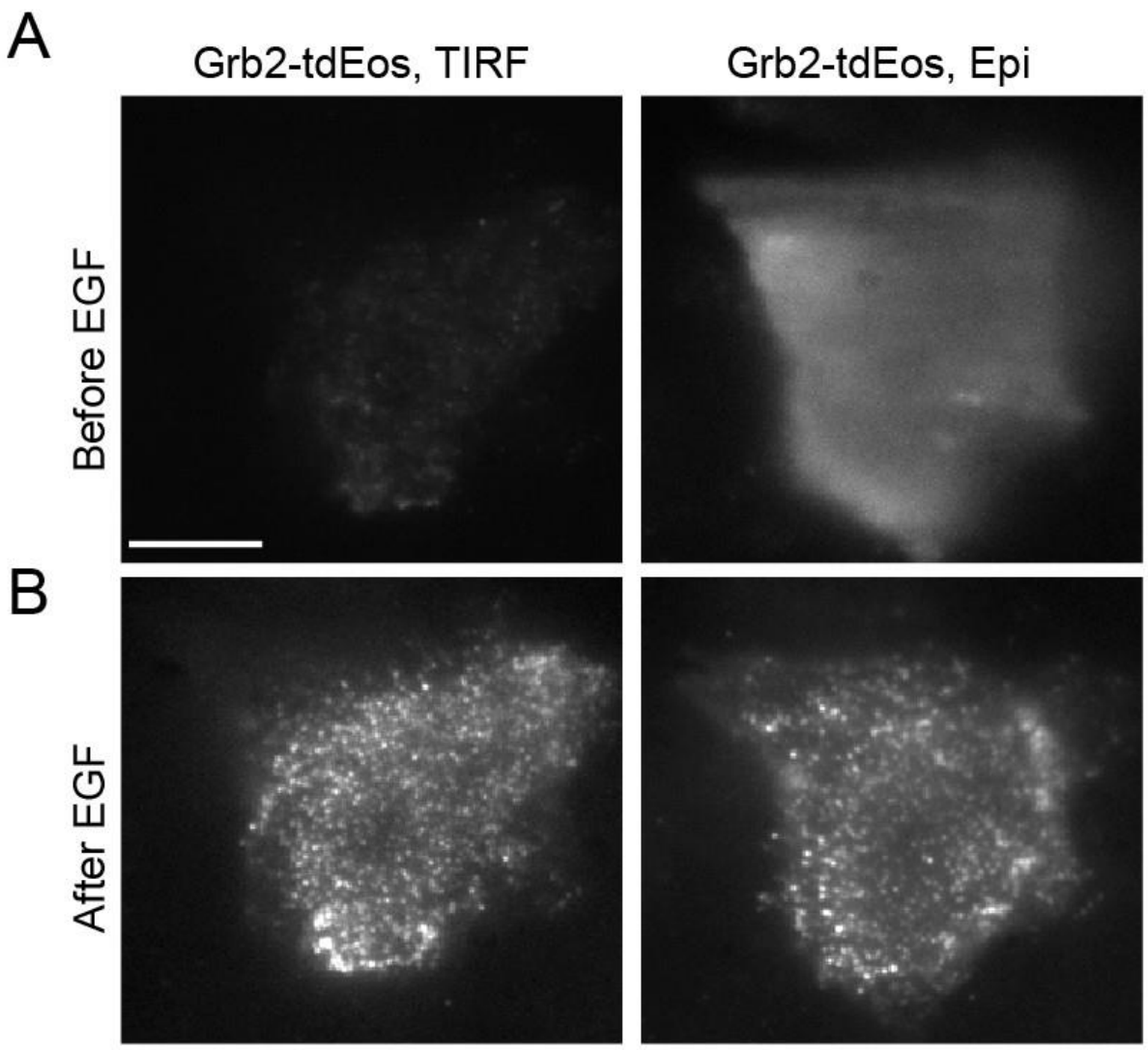

Figure S9. Substantial translocation of Grb2-tdEos from cytoplasm to plasma membrane upon EGF stimulation. (A) Overexpressed Grb2-tdEos molecules are significantly present in the cytoplasm with no signal at TIR- and diffuse fluorescence signal at epi-illumination. (B) Upon EGF, Grb2-tdEos molecules were significantly translocated to the plasma membrane visualized by both TIR and epi-illumination.

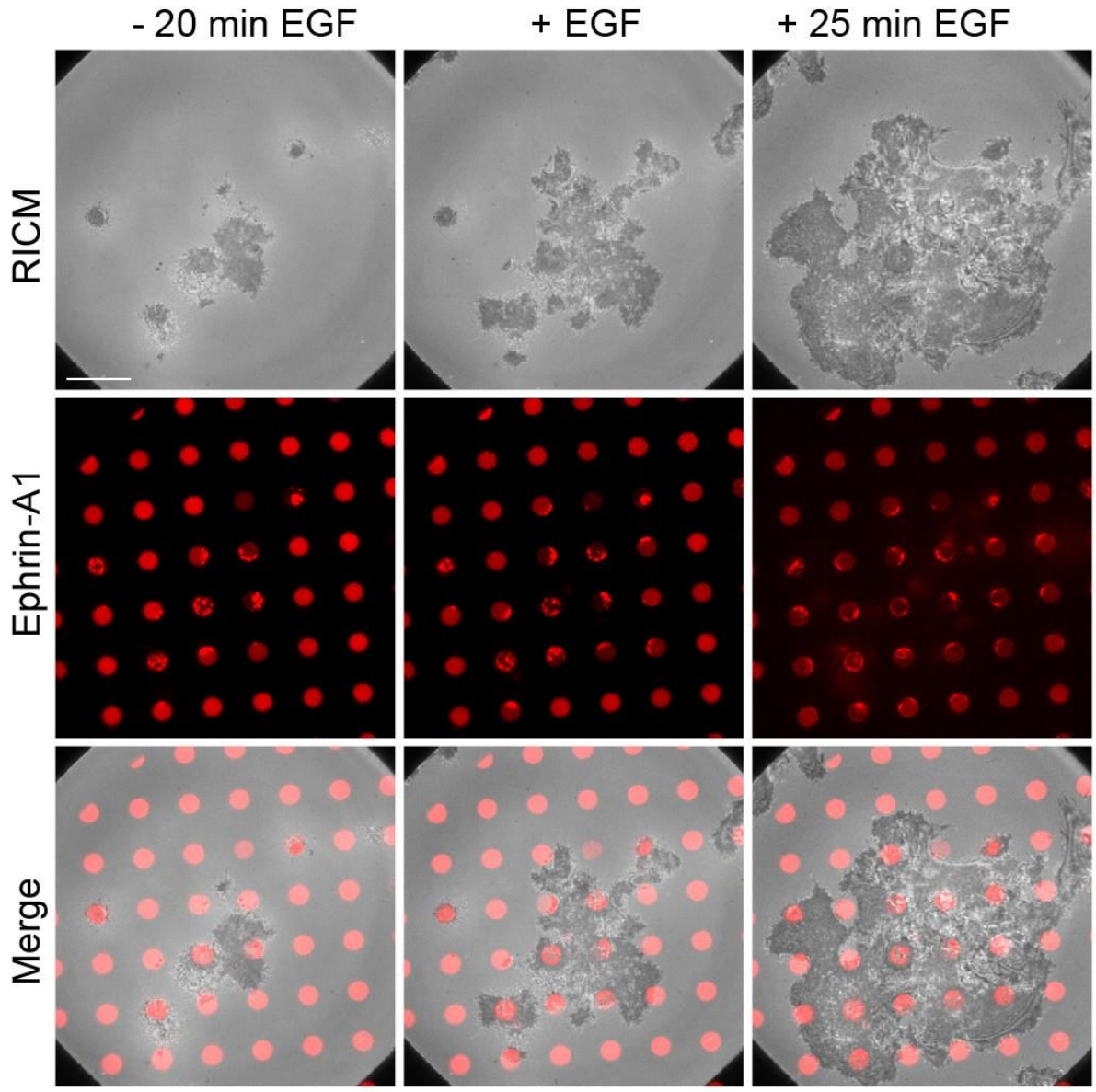

Figure S10. Ephrin-A1:EphA2 clustering is not affected by EGF stimulation. MDA-MB-231 cells stimulated with EGF during spreading on ephrin-A1 functionalized membrane array surfaces. Prior to the addition of EGF (first column), ephrin-A1 clusters can be observed beginning to form. Upon EGF stimulation (second column) and at 25 min after the initial introduction of EGF (third column), ephrin-A1 clustering was consistently observed in the same manner of cell spreading without EGF shown in Figures 1 G, 2 A-B and 5 A, indicating that ephrin-A1:EphA2 clustering was independent of EGF stimulation.

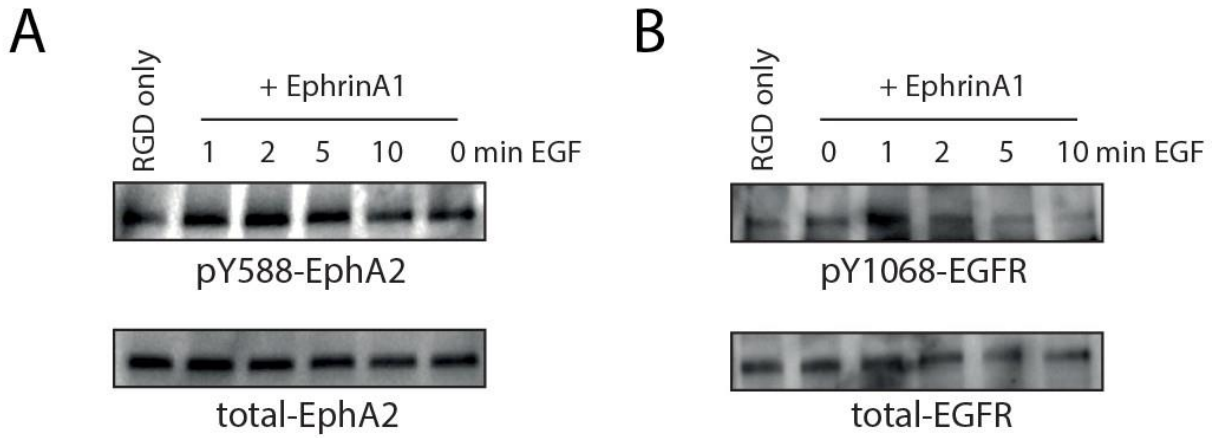

Figure S11. EGF-independent EphA2 activation. Western blots of MDA-MB-231 cells for EphA2 phosphorylation using pY588 anti-phosphotyrosine antibodies (A) and EGFR phosphorylation using pY1068 anti-phosphotyrosine antibodies (B) upon 50 ng/ml of EGF. There was no significant change in pY-EphA2, but a significant increase in pY-EGFR was detected.

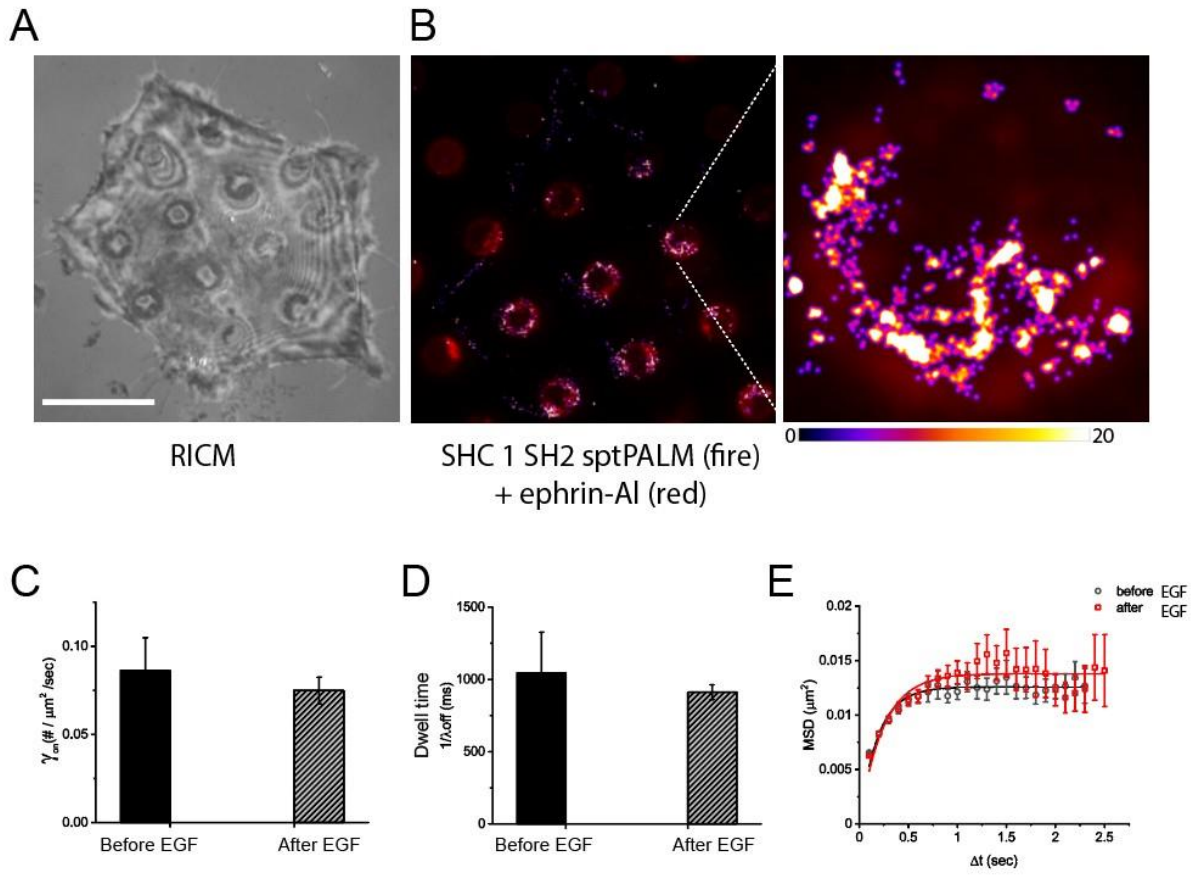

Figure S12. SHC1 SH2 domain dynamics in ephrin-A1:EphA2 clusters are not affected by EGF stimulation. (A) RICM image of MDA-MB-231 cells expressing SHC1 SH2-tdEos spread on ephrin-A1-Alexa 680 SLB hybrid substrate. (B) sptPALM image of SHC1 SH2-tdEos (fire color) after EGF superimposed with ephrin-A1 SLB (red) shows the localization of SHC1 SH2 molecules with ephrin-A1 clusters in SLB corrals. The scale bar in enlarged SLB (right panel) represents the total number of events per pixel. A PSF with 50 nm FWHM was used and sub-pixelized by 10x. (C) The number of SHC1 SH2-tdEos new binding in SLBs per second before and after EGF (80 ng/ml). Six time-lapse single molecule movies from 2 cells each were used for this analysis. The mean γ_{on} are 0.08 (ME:0.01) (#/μm^2/sec) and 0.07 (ME: 0.007) (#/μm^2/sec) for before and after EGF, respectively. (D) Mean dwell time of SHC1 SH2-tdEos in ephrin-A1-SLBs before (1043 (± 283) ms) and after EGF (910 (± 52 ms) (n = 2 cells, n = 6 movies). (E) MSD-dt of SHC1 SH2 using all trajectories before (black) and after (red) EGF. Scale bar, 10 μm.

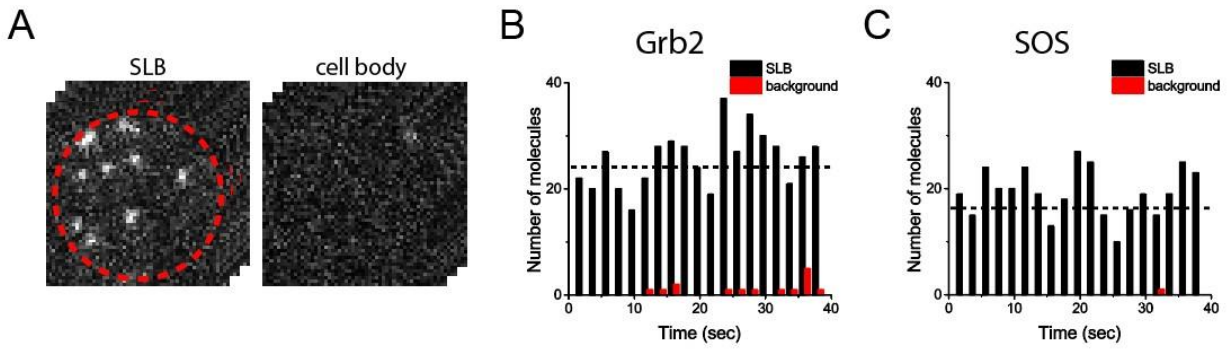

Figure S13. Steady-state of Grb2 and SOS membrane kinetics before EGF. (A) Time-lapse image sequences of Grb2-tdEos in ephrin-A1 SLB (left) and background (right) cropped from a single-molecule movies (Movie 9). (B - C) Time-dependent number of newly appeared Grb2-tdEos (B) and SOS-mEos3.2 (C) in SLB (black) and background (red) in the absence of EGF. Movie was taken 10 Hz and binned for 2 sec. Relatively steady state of new binding event is achieved.

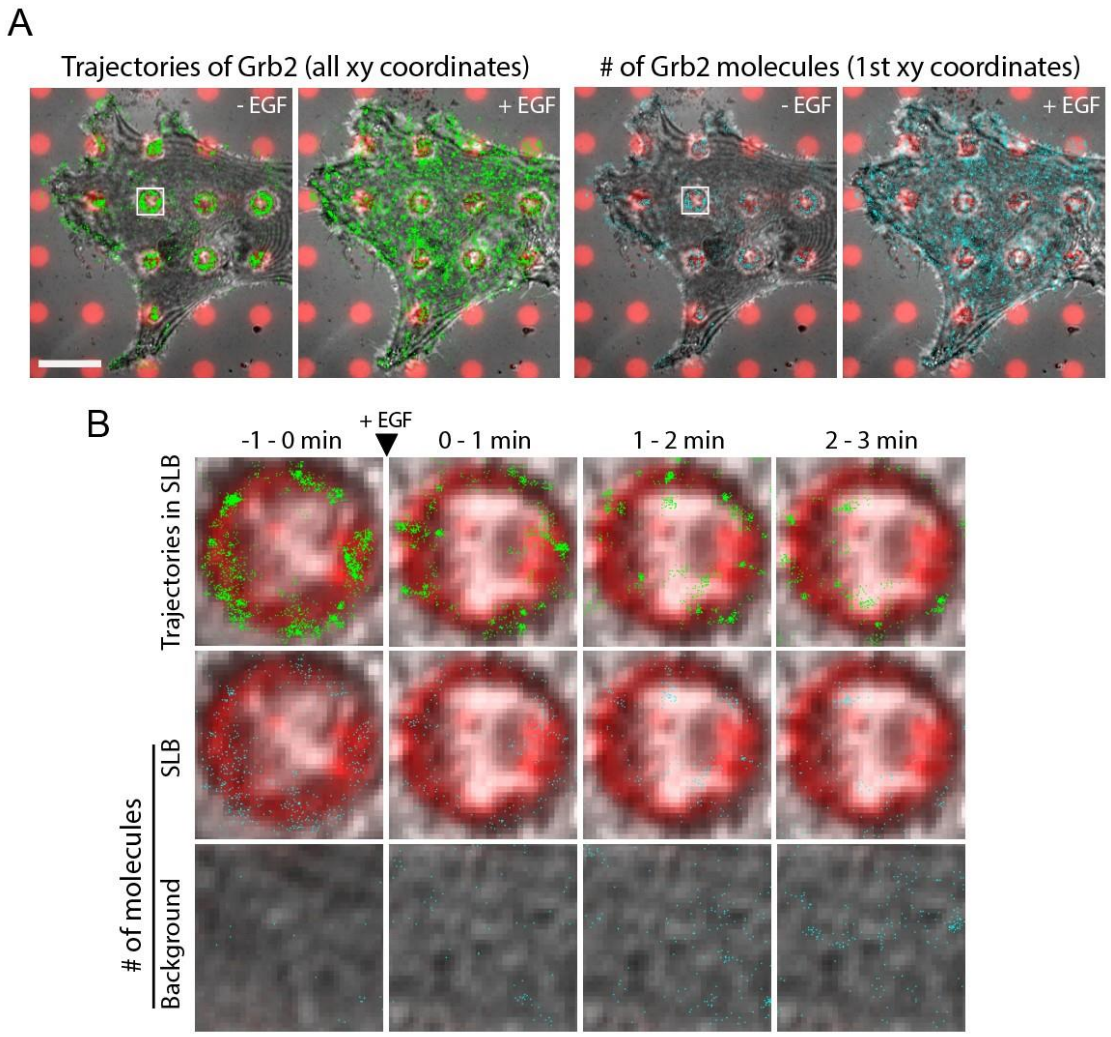

Figure S14. Time-dependent single-molecule localization of Grb2-tdEos before and after EGF. (A) Left panels: merged between RICM image of MDA-MB-231 (gray), epifluorescence image of ephrin-A1 SLB (red), and reconstructed-dot image of xy coordinates (green dots) of all Grb2-tdEos events before (left) and 2 min after EGF (right). Right panels: merged between RICM (gray), ephrin-A1 SLB (red), and reconstructed-dot image of first xy coordinates (cyan dots) from all Grb2-tdEos trajectories before (left) and 2 min after EGF (right). (B) Magnified images of all xy coordinates (first row), and the first xy coordinates from trajectories (second and third rows) in the SLB (second) and background (third). Time-dependent localization image sequences show globular dissociation of Grb2 from SLBs and simultaneous association in the background after EGF. Movie 10 was used for this analysis. Scale bar, 10 μm.

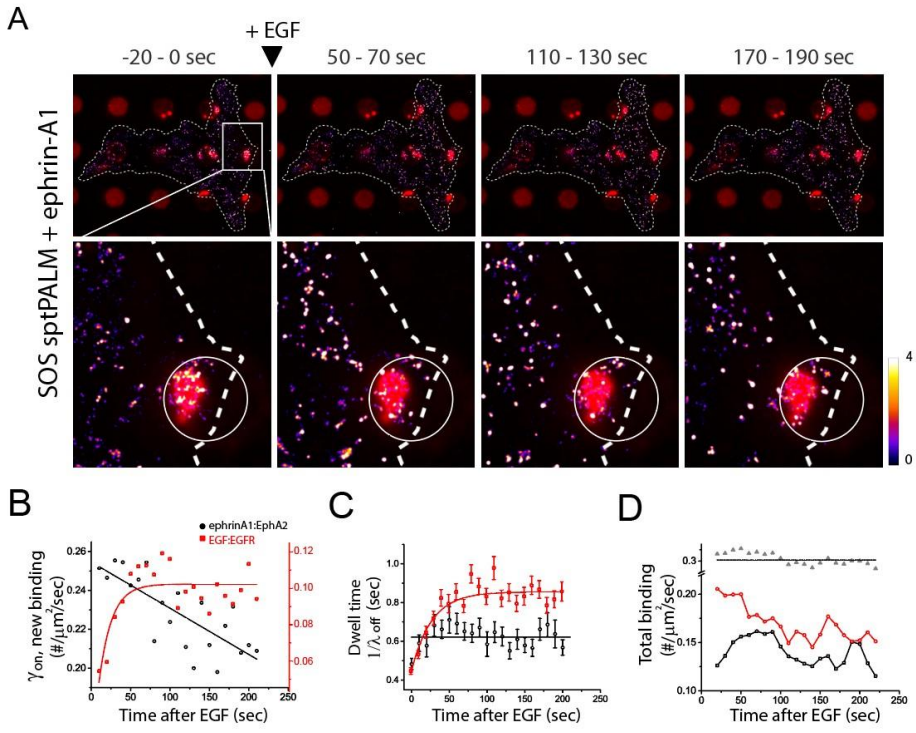

Figure S15. Single molecule kinetics measurements recapitulate SOS mass flow from ephrin-A1:EphA2 clusters to newly formed EGF:EGFR clusters. (A) The SOS-mEos3.2 sptPALM image sequences (fire color) superimposed with the eprhinA1-Alexa 680 SLBs (red) show a gradual decrease in SOS-mEos3.2 signal in SLBs (equivalent to ephrin-A1:EphA2 complex) and a simultaneous increase in the background (equivalent to EGF:EGFR complex) after 80 ng/ml of EGF. The 2D xy coordinates of all trajectories (except 1 frame length) were replaced with PSF with 0 - 1 gray values and 50 nm FWHM and then integrated for every minute. A portion of the single-molecule movie used here is shown in Movie 11. (B) Time-dependent new binding rate, $\gamma_{on}(t)$, of SOS-mEos3.2 per area in SLB (black) and background (red) after EGF. (C) Time-dependent mean dwell time, $1/\lambda_{off}(t)$, of SOS-mEos3.2 in ephrin-A1:EphA2 (black) and EGF:EGFR clusters (red). The $1/\lambda_{off\text{-}EphA2}(t)$ fluctuated slightly against 650 ms, but $1/\lambda_{off\text{-}EGFR}(t)$ gradually increased to saturate 1000 ms. (D) Computed total binding of SOS-mEos3.2 using measured $\gamma_{on}(t)$ and $\lambda_{off\text{-}EGFR}(t)$ with Eq3 (see above Supporting material) in eprhinA1:EphA2 (black) and EGF:EGFR clusters (red). The curves recapitulate the asymmetric kinetics of SOS by at least 1 min. In this region, SOS binding decreased in ephrin-A1:EphA2 but increased in the EGF:EGFR over time. The sum of membrane signal of SOS-mEos3.2 (gray dotted line) did not change significantly, implying the SOS mass flow from the EphA2 signaling complex to EGFR signaling complex after EGF.

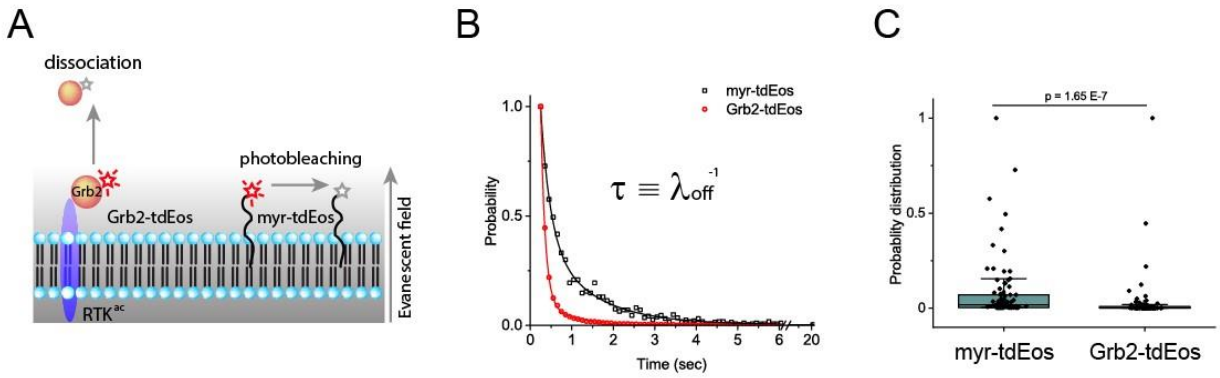

Figure S16. Experimental criteria for Grb2 single molecule dwell time measurement. (A) The schematic diagram for detecting Grb2-tdEos dissociation from membrane-bound phosphorylated-RTK. The binding time of Grb2-tdEos in phosphorylated-RTK should be shorter than the photobleaching time of tdEos tagged with myristoylation membrane tag. (B) The normalized distribution of individual Grb2-tdEos dwell time (red) and myr-tdEos photobleaching time (black). Statistically, the tdEos photobleaching time was significantly longer than Grb2-tdEos-RTK dwell time. (C) Testing the difference of the population means lead to p-value of 1.6E-7. Here we defined the characteristic time constant, τ, as the mean dwell time of Grb2-tdEos, λ_{off}^{-1}.

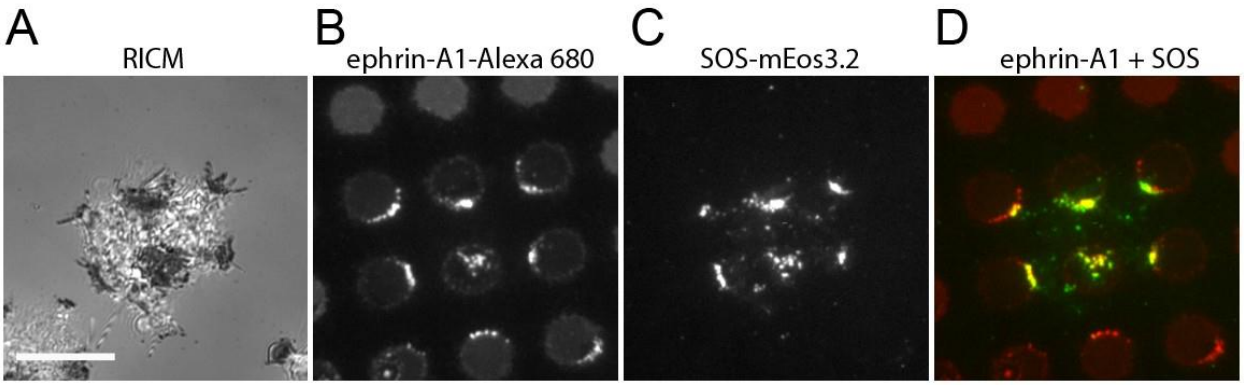

Figure S17. SOS recruitment at ephrin-A1:EphA2 clusters in MCF-10A. (A) RICM image of MCF-10A cells expressing SOS-mEos3.2 spreading on an ephrin-A1 SLB hybrid substrate. (B) Epifluorescence of ephrin-A1-Alexa 680 clusters in cell contacted SLBs. (C) Ephrin-A1:EphA2 clusters recruitment of SOS-mEos3.2. (D) Colocalization of ephrin-A1-Alexa 680 (red) and SOS-mEos3.2 (green) signals. Scale bar, 10 μm.

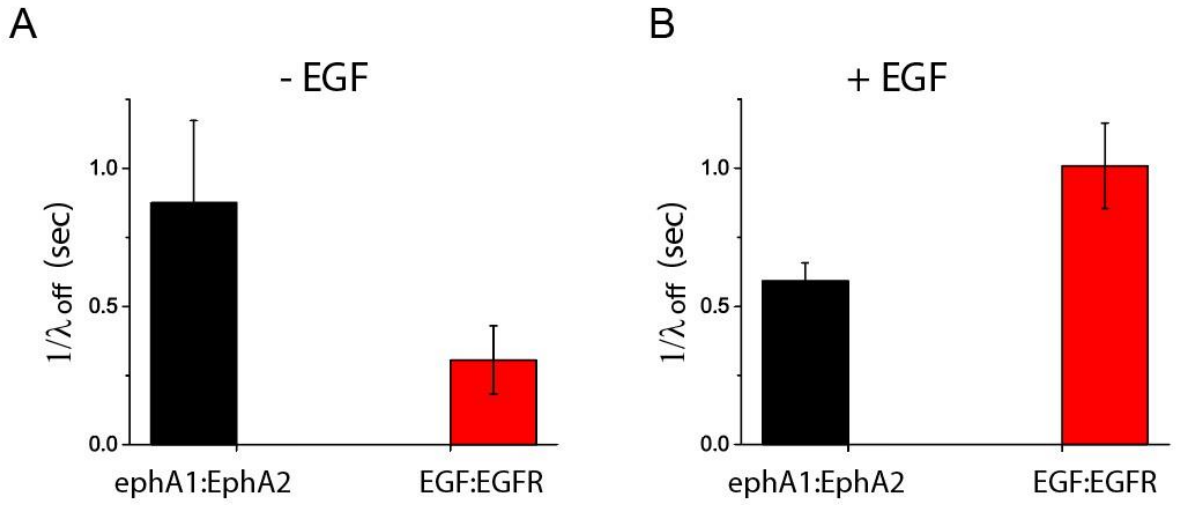

Figure S18. Dwell time of Grb2 in ephrin-A1:EphA2 and EGF:EGFR clusters of MCF-10A. (A -B) Mean dwell time of Grb2-tdEos in ephrin-A1:EphA2 clusters (black) and in EGF:EGFR clusters (red) in the absence (A) and presence of EGF (B). Mean values are; 876 (ME:29) ms in ephA1:EphA2 and 306 (ME:12) ms in EGF:EGFR before EGF, and 592 (ME:6) ms in ephA1:EphA2 and 1008 (ME:15) ms in EGF:EGFR after EGF, respectively. Two cells and several time-lapse movies were used for this analysis.

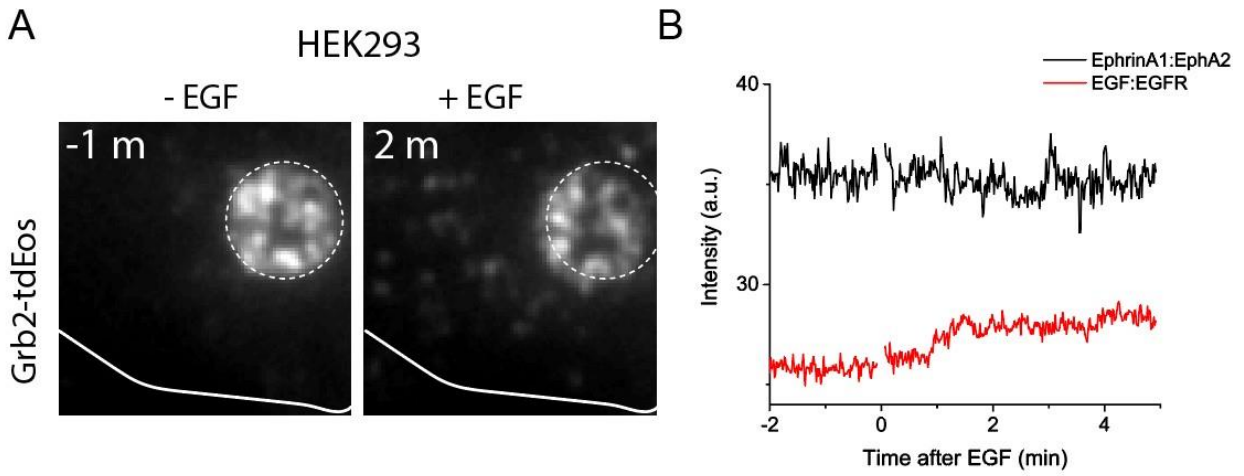

Figure S19. No Grb2 depletion from ephrin-A1:EphA2 clusters by EGF stimulation in HEK293 cells. (A) Fluorescence images of HEK293 cells (white line for cell boundary) expressing Grb2-tdEos spread on ephrin-A1 SLB hybrid substrate show a strong membrane signal of Grb2-tdEos before EGF (left), which remains unchanged after 80 ng/ml of EGF (right). HEK293 is known to express a significantly lower amount of EGFR compared to EphA2. The whole-cell movie is shown in Movie 14. (B) Intensity profiles of Grb2-tdEos in SLB (black, EGF:EGFR clusters) and background (red, EGF:EGFR clusters).

Movie Legends

Movie 1. Ephrin-A1:EphA2 clustering on SLB corrals does not affect EGFR diffusion in MDA-MB-231 cells. Time-lapse TIRF images of an MDA-MB-231 cell expressing EGFR-mEos3.2 interacting with ephrin-A1 functionalized SLB corrals (highlighted in Figure S2) reveal similar EGFR diffusion inside and outside SLB corrals. Trajectories and MSD-Δt curves are shown in Figure S2. The video was taken at 10 fps.

Movie 2. Multi-channel time-lapse imaging of MDA-MB-231 cells expressing Grb2-tdEos interacting with ephrin-A1 functionalized SLB micropatterned substrate. The multi-channel movies show cell initial spreading and SLB-contact (RICM, first panel), ephrin-A1 clustering at SLB-cell contact (second), Grb2 recruitment to ephrin-A1 clusters (third) and colocalization between ephrin-A1 and Grb2 (merge, last). The time interval between image sequences was 10 sec and the time lag between channels was less than 1 sec. These movies were used for analysis in Figure 2 A and Figure S3.

Movie 3. Multi-channel time-lapse imaging of MDA-MB-231 cells expressing SOS-mEos3.2 interacting with ephrin-A1-functionalized SLB micropatterned substrate. The multi-channel movies show cell initial spreading and SLB-contact (upper left), ephrin-A1 clustering at SLB-cell contact (upper right), SOS recruitment to ephrin-A1 clusters (lower left) and colocalization between ephrin-A1 and SOS (lower right). The time interval between image sequences was 30 sec and the time lag between channels was less than 1 sec. These movies were used for analysis in Figure 2 B.

Movie 4. EGF stimulation causes Grb2 depletion from the ephrin-A1:EphA2 clusters and simultaneous formation of a new EGF:EGFR:Grb2 complexes on the membrane. MDA-MB-231 cell expressing Grb2-tdEos spread on ephrin-A1-Alexa 680-functionalized SLB micropatterned substrate. The pre-localized Grb2-tdEos fluorescence signals in SLBs abruptly decrease upon the addition of 80 ng/ml of EGF (third image frame). Simultaneously, Grb2-tdEos signals in the background immediately increased as puncta through the membrane of the cell. The right panel shows a merged image of ephrin-A1-Alexa 680 (red) with Grb2-tdEos (green) cropped from the left cell in left panel. SLB size is 3 μm in diameter. This movie was used for analysis in Figure 3.

Movie 5. EGF stimulation reduces Grb2-tdEos signals in SLB without affecting ephrin-A1-Alexa 680 signaling. A group of the cropped SLBs from the time-lapse movie before and after EGF. The size of SLB is 2 μm in diameter. EGF was added at the 5^{th} frame.

Movie 6. EGF stimulation causes SOS depletion from the ephrin-A1:EphA2 clusters and simultaneous formation of a new EGF:EGFR:SOS complexes on the membrane. MDA-MB-231 cells expressing SOS-mEos3.2 (middle panel) spread on ephrin-A1-Axlex 680 coated SLBs (left). Upon addition of 80 ng/ml of EGF at t = 0, SOS-mEos3.2 signal abruptly decreases in SLB corrals with a simultaneous increase in outside of SLB with puncta. Ephrin-A1-Alexa 680 signal in SLB remained unchanged after EGF. SLB size is 3 μm in diameter. This movie was used for analysis in Figure S7.

Movie 7. EGF stimulation reduces SOS-mEos3.2 signals in ephrin-A1 SLB. A group of the cropped SLB from SOS-mEos3.2 time-lapse movie before and after EGF. The boundaries of SLBs were highlighted with white circles. The number of SOS-mEos3.2 clusters or molecules decreased over EGF stimulation time.

Movie 8. SHC1 binding of the ephrin-A1:EphA2 clusters is not affected by EGF stimulation. MDA-MB-231 cells expressing SHC1 SH2-tdEos (green) spread on ephrin-A1-Alexa 680 coated

SLB patterns (red). SHC1 SH2-tdEos molecules are recruited to ephrin-A1:EphA2 clusters in SLBs, which remain almost similar after EGF (80 ng/ml) at t = 0. SLB size is 3 μm in diameter. Intensity analysis has shown in Figure 4 D.

Movie 9. Equilibrium single molecule kinetics of Grb2 and SOS in the ephrin-A1:EphA2 clusters. Grb2-tdEos binding/unbinding in the SLB (left panels: first) and in the background (left panels: second), and SOS-mEos3.2 in the SLB (right panels: first) and in the background (right panels: second). Individual Grb2 and SOS molecules consistently bind and unbind in the SLBs, but these events were significantly suppressed in the background. The movie was recorded at 20 Hz with TIRF. Quantification is shown in Figure S13 B-C.

Movie 10. Time-lapse, single molecule imaging shows changes in Grb2 binding/unbinding kinetics before and after EGF in the ephrin-A1:EphA2 and EGF:EGFR signaling complexes. MBA-MD-231 cells expressing Grb2-tdEos spread on ephrin-A1-functionalized SLB micropatterns (red, in the first image) substrate. EGF was added at t = 0, and on/off events are continuously imaged at 10 Hz for few minutes. The movie shows that the frequent Grb2-tdEos on/off events in SLB progressively decreases after EGF but simultaneously increase throughout the cell, indicating that EGF-induced EGFR activation competitively recruits Grb2. SLB size is 3 μm in diameter. This movie was used for quantifications in Figure 5.

Movie 11. Time-lapse, single-molecule imaging shows changes in SOS binding/unbinding kinetics before and after EGF in ephrin-A1:EphA2 and EGF:EGFR signaling complexes. MBA-MD-231 cells expressing SOS-mEos3.2 spread on ephrin-A1 coated SLBs (red, in the first image) substrate. EGF was added at t = 0, and on/off events are continuously imaged at 10 Hz for few minutes. The movie shows that the frequent SOS-mEos3.2 on/off events in SLB progressively decrease after EGF but simultaneously increase throughout the cell, indicating that EGF-induced EGFR activation competitively recruits SOS. SLB size is 3 μm in diameter. This movie was used for quantifications in Figure S15.

Movie 12. Grb2 is not depleted in the ephrin-A1:EphA2 clusters with EGF in MCF-10A cells expressing far less EGFR than EphA2. MCF-10A cells (upper left) expressing Grb2-tdEos (lower right) spread on ephrin-A1-Alexa 680-SLB (upper right). Merged image (lower left) shows initial strong and colocalized Grb2 signals with ephrin-A1 clusters in SLBs, which remain almost unchanged after EGF (20 ng/ml) at t > 0. However, Grb2-tdEos puncta appeared continuously throughout the membrane after EGF, indicating EGF-induced EGFR activation. SLB size is 3 μm in diameter. Quantification is shown in Figure 6 B - C.

Movie 13. High dose of EGF still does not reduce Grb2 binding in the ephrin-A1:EphA2 clusters of MCF-10A cells. MCF-10A cells expressing Grb2-tdEos (green, single molecules) begin to spread over ephrin-A1-Axlex 680-SLB (red) hybrid substrate. In the middle of time-lapse TIRF imaging, 80 ng/ml of EGF was introduced rapidly at t = 190 sec. The movie shows no significant change in Grb2 binding/unbinding in cell-contact SLBs before and after EGF, whereas the membrane signaling of Grb2-tdEos increased slightly after EGF in this early spreading cell.

Movie 14. EGF stimulation does not cause depletion of Grb2 from ephrin-A1:EphA2 clusters in HEK293 cells that express relatively high levels of EphA2 than EGFR. HEK293 cells expressing Grb2-tdEos spread on ephrin-A1-SLB substrate (red in the first image) and accumulated in the ephrin-A1 clusters in the SLBs. This Grb2 signals did not change much after EGF (t > 0), while slightly increasing in the background. The quantification has shown in Figure S18. SLB size is 3 μm in diameter.

Supporting References

1. J. A. Jadwin *et al.*, Time-resolved multimodal analysis of Src Homology 2 (SH2) domain binding in signaling by receptor tyrosine kinases. *Elife* **5**, e11835 (2016).
2. Y. Sako, T. Yanagida, Single-molecule visualization in cell biology. *Nat Rev Mol Cell Biol* Suppl, SS1-5 (2003).
3. D. Oh *et al.*, Fast rebinding increases dwell time of Src homology 2 (SH2)-containing proteins near the plasma membrane. *Proc Natl Acad Sci U S A* **109**, 14024-14029 (2012).